Using the S^4 software to optimise the design process of reflective epsilon-near-zero metasurfaces

Laidlaw research project by Sofya Dobrynina, supervised by Dr. Sebastian Schulz

School of Physics and Astronomy, University of St Andrews, North Haugh, St Andrews, Fife KY16 9SS, UK
(August 2021)

1 Introduction

In our current fast-paced and technologically centred world, the scientific frontier is constantly pushed further in the search of new discoveries and innovations. Optical physics is no exception. With so much of modern technology being dependent on optics, including fibre-optic technology for telecommunications [1], and biomedical imaging [2] just to name a few, it is no wonder why this field is so heavily researched. But despite already having well-developed optical technologies at our fingertips even in our daily lives, there is always room for improvement. And this potential for considerably rapid progress can be provided by epsilon-near-zero (ENZ) metasurfaces. A relatively recent development, ENZ metasurfaces have demonstrated a strong nonlinear response, enhancing the optical qualities of instruments that implement them [3]. However, the design process of these metasurfaces is currently long and cumbersome due to the accurate but slow finite-difference time-domain (FDTD) method of simulation, thus delaying their development and wider use in technology. This paper looks to test how accurately the spectra from ENZ metasurfaces can be reproduced in the S^4 software, which employs another simulation method called Fourier Modal Method (FMM), and consider this software as a useful tool for the optimisation of the design process of these surfaces.

2 What are ENZ metasurfaces?

Before beginning simulation, it is vital to understand what ENZ metasurfaces are and how they operate. An epsilon-near-zero material is one whose real part of the permittivity is close to or crosses zero within a certain wavelength range which differs with different materials exhibiting this property. At the same time, the imaginary part of the permittivity remains finite and above zero. It is within this ENZ wavelength range that the materials exhibit interesting optical properties, for example, the phase velocity of the wave tends to infinity, and the phase and amplitude of the wave remain almost constant (with slow modulations) inside the material [4]. As well as this, ENZ materials have demonstrated a strong nonlinear optical response [3], making their application in photonics and optical technologies very desirable and sought after.

In turn, a metasurface is a planar surface of subwavelength thickness containing in-plane features,

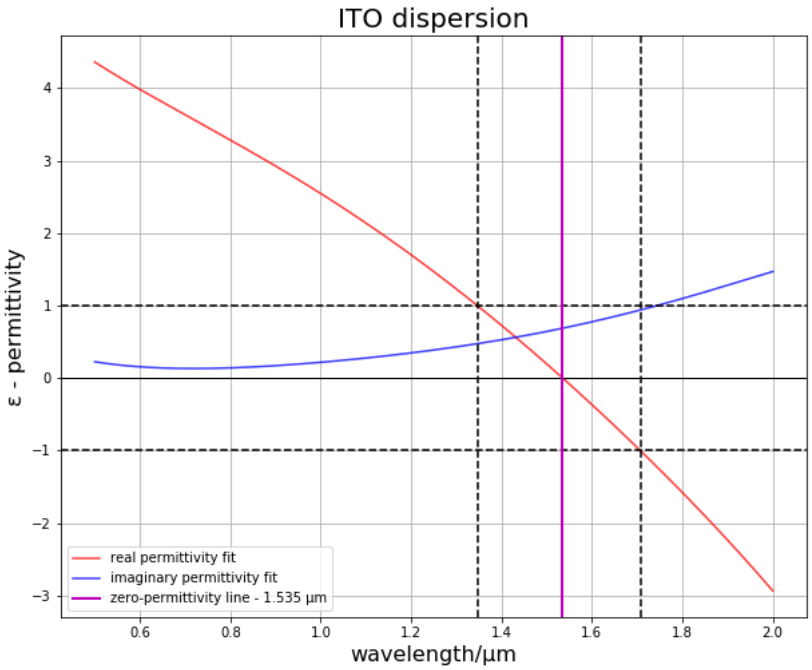

Figure 1: *The real and imaginary permittivities of the ITO material used in this investigation. The black dashed lines show the points on the graph where* $-1 < \epsilon < 1$*, and we can clearly see where the real permittivity crosses the zero-line. These curves are polynomial fits to the data provided by Laura Wynne.*

and which displays an inhomogeneous phase distribution for the electromagnetic waves incident on it [5]. This is usually achieved by optical antennae (or other light scatterers) being placed periodically in arrays on the surface of some spacer, and these scatterers can take different shapes, sizes, and orientations, and made of different materials depending on the design purpose of the metasurfaces [6]. The shape and orientation of each antenna determine how it interacts with light and the phase that it imprints, allowing us to better control the wavefront for a variety of optical purposes (transmission, reflection, etc). In addition, metasurfaces prove to be superior to traditional equipment, such as lenses, due to their small size, making them useful for the optimisation of optical instruments and devices.

The wave control provided by metasurfaces is based on the Huygens-Fresnel principle: each point on a wavefront acts as its own source of waves originating from that point. At each point that the primary wave is incident on the surface interface, a secondary source of circular wavefronts is produced. From this, the generalised Snell's law can be derived [7]:

$$n_t sin(\theta_t) - n_i sin(\theta_i) = \frac{\lambda_0}{2\pi} \frac{d\phi}{dx} \tag{1}$$

The symbols in equation (1) correspond to those shown in **Figure 2**. Here, the n_i and n_t represent the refractive indices of the two media that the wave travels through; λ_0 is the free-space

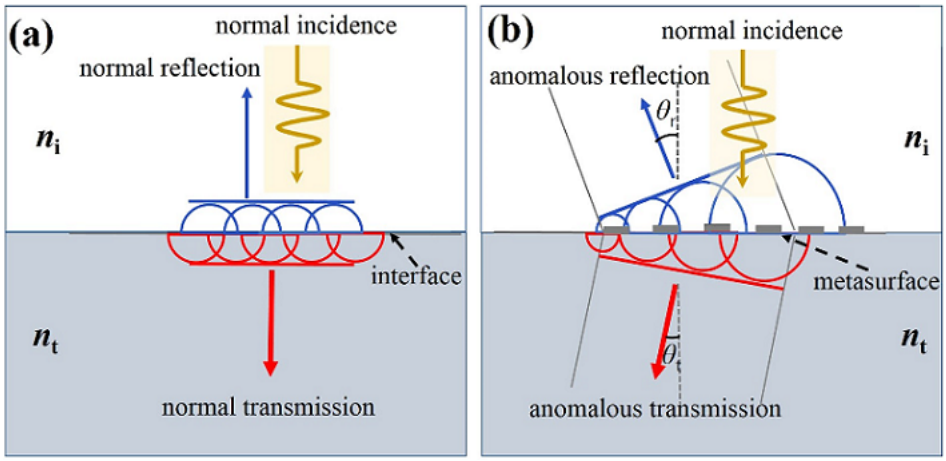

Figure 2: *A representation of the Huygens-Fresnel principle acting on* ***a)*** *a non-modified interface;* ***b)*** *an interface with a metasurface; between two homogeneous media. The figure is adapted from [7].*

wavelength; θ_i, θ_t, θ_r represent the angles of incidence, transmission, and reflection respectively; and ϕ represents the phase response. We see that the angles of transmission and reflection are dependent on the phase gradient with position, which is achieved by the scatterers incorporated into the metasurface, leading to different transmission and reflection than for non-modified interfaces.

3 Different simulation methods

When simulating the optical properties and spectra obtained from metasurfaces, we compute and solve a series of Maxwell's equations relating to our particular system to obtain the required results. There exist different methods of numerically solving Maxwell's equations, but this paper will focus only on two: the finite-difference time-domain method (abbreviated as FDTD), and the Fourier modal method (FMM).

The FDTD method is perhaps the most accurate and popular method of simulating spectra obtained from metasurfaces. It belongs to a group of methods termed as the space domain methods, in which Maxwell's equations are given as partial differential equations, and numerical values of the field are computed at each discretized spatial point of the simulated system [8]. The fields are computed in time increments by "updating" the equations of present fields in terms of the past field, thus taking the computation forward in time [9]. Although accurate, this computational method is very slow, with equations having to be solved at every point in the structure. Consequently, for large structures, the FDTD method can take days to compute a simulation.

By contrast, the FMM method belongs to the class of spatial frequency domain methods, wherein Maxwell's equations are transformed into algebraic Maxwell eigenvalue equations. A complete set of eigenmodes for the system can be found from these equations, and these span the entire dimension of the optical structure at hand [10]. As this eigenmode matrix is constructed over the whole of the structure span, instead of having to solve an equation at every point in the structure, FMM

simulation is computed much faster than the FDTD. However, some accuracy is lost for this same reason.

The S^4 software explored in this investigation implements the FMM to solve Maxwell's equations through layered periodic structures [11], and so is expected to produce less accurate simulations than those produced in the FDTD simulations. But by comparing the S^4 simulations to the already-existing FDTD simulations of identical structures, we can determine how accurately S^4 can simulate the same results, and determine whether it can optimise the design process of ENZ metasurfaces by its fast simulation time.

4 The S^4 software

4.1 S^4 basics

The S^4 software is fronted by the Lua programming language, and although a Python extension can be used to code structures within the software, it is preferrable to use the former language, since the software is predisposed for its use. To begin the simulation, a standard block of code is written which defines the lattice (the simulation region), the number of Fourier expansions to be used in the simulation, the materials used, the structure of the surface, and the direction of the incident wave. The base unit length used in all simulations was a micron, and the surface dimensions inputted accordingly.

For the purpose of this investigation, the primary wave is defined as normally incident (angles θ and ϕ both equal to 0), and p-polarised (polarised parallel to the plane of incidence), as this is defined as the x-direction in S^4. Since our antenna dimensions are longer in the x-axis than in the y-axis, we have to set the wave polarisation along the x-axis as well. The incident wave has initial phase of 0.

4.2 Varying material dispersion

Although the materials defined in the code shown in **Figure 3** seem to have constant values of real and imaginary permittivity, this is not in fact the case. The main materials used in the simulations were gold (Au), zirconia (ZrO2), indium tin oxide (the ENZ material - ITO for short), and glass. While glass has a constant permittivity, the real and imaginary permittivities of the three former materials vary with wavelength, and so a "for" loop must be constructed so that each wavelength iteration in the simulation would have the correct dispersion value associated with it.

The dispersion data for gold and zirconia were taken from Johnson and Christy [12], and Wood and Nassau [13], respectively. The ITO dispersion data (as well as the antenna and surface dimensions) was provided by Laura Wynne. The former two data sets had to be converted into values of permittivity, since they were originally given in terms of their complex refractive index: $n + i\ k$. This was done using the standard conversion formula for real and imaginary permittivities, namely:

$$\epsilon_r = n^2 - k^2 \tag{2}$$

```
----------S4 simulation---------------

S= S4.NewSimulation()
S:SetLattice({0.6,0},{0,0.6}) --in micrometres
S:SetNumG(300)


--all materials to be considered, defined through real and imaginary permittivities
S:AddMaterial("Vacuum",{1,0})
S:AddMaterial("Glass",{2.1,0})
S:AddMaterial("Air",{1,0})
S:AddMaterial("Gold",{-10,1})
S:AddMaterial("ITO",{3.3,0.14})

--setting layers' order and thickness and defining antenna dimensions
S:AddLayer("AirAbove",0,"Vacuum")
S:AddLayer("Gold_Antenna",0.04,"Air")
S:SetLayerPatternRectangle("Gold_Antenna","Gold",{0,0},0,{0.21,0.0845})
S:AddLayer("Glass_Spacer",0.025,"Glass")
S:AddLayer("ITO_layer",0.02,"ITO")
S:AddLayer("Glass_Spacer",0.05,"Glass")
S:AddLayer("Backreflector",0.005,"Gold")
S:AddLayerCopy("Substrate",5,"Glass_Spacer")

--setting normally incident p-polarized wave
S:SetExcitationPlanewave({0,0},{0,0},{1,0})
```

Figure 3: *An example start code for a simulation. In the above example, the simulation region encompasses 600×600 nm, the number of Fourier expansions used is 300.*

$$\epsilon_i = 2nk \tag{3}$$

Polynomial fits to the dispersion data were produced in Python, and these were then inputted into Lua in the form of arrays, which were subsequently transformed into functions to be used in the "for" loop to ensure the correct simulation.

4.3 Table of dimensions

Below is a table listing all of the antenna, layer, and simulation region dimensions used in the following S^4 simulations intended for comparison with the corresponding FDTD simulations.

Table of dimensions			
Dimensions/μm	Au on glass without ITO	ZrO_2 on glass without ITO	Au on glass with ITO
Antenna x-length	0.476	0.7	0.42
Antenna y-length	0.194	0.2	0.169
Antenna thickness	0.04	0.87	0.04
ITO layer thickness	N/A	N/A	0.02
Glass spacer thickness	arbitrary	arbitrary	0.05
Gold back-reflector thickness	N/A	N/A	0.005
Simulation region	0.6 x 0.6	1.05 x 0.7	0.6 x 0.6

5 Simulations with S^4

5.1 Running the simulation without the ITO layer

Before the simulation could be run with the ITO layer in the structure, a control run had to be made of how accurately S^4 computed the transmission spectra of simple surfaces, namely the gold and dielectric antennae on a glass spacer, to the corresponding FDTD simulations. This involved the antennae in question being placed on a glass spacer of arbitrary thickness without further additions to the surface. For these simulations, a lesser number of Fourier expansions was used than for simulations including the ITO layer due to the simplicity of the structures, with 110 and 90 expansions used for the gold and zirconia antennae respectively.

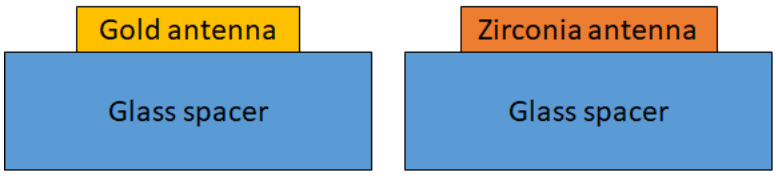

Figure 4: *Schematic of the simplest structures to perform a control simulation*

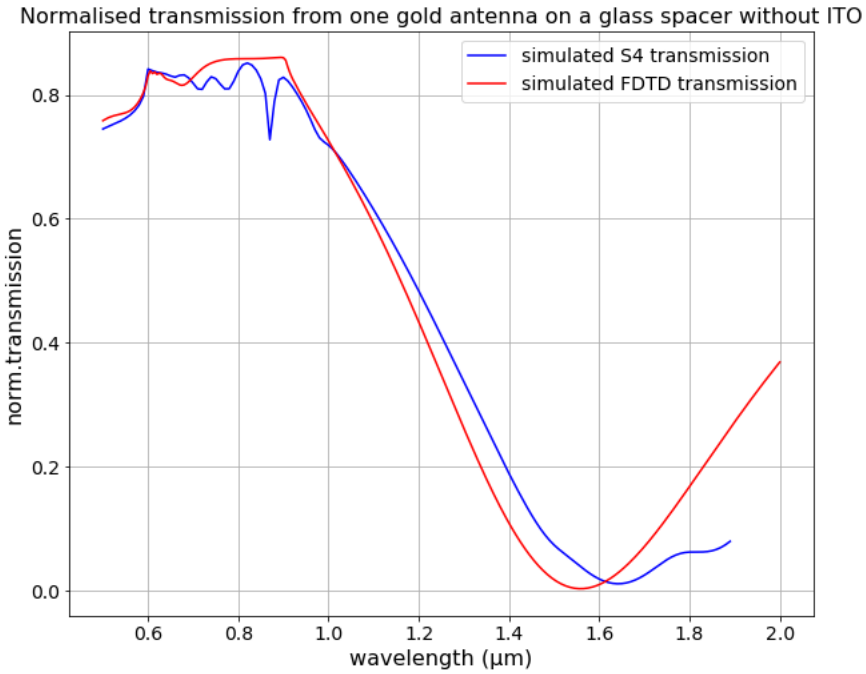

Figure 5: *Normalised transmission from one gold antenna on a glass spacer*

From **Figures 5 and 6**, we can clearly see that the S^4 simulated normalised transmission matches the FDTD simulation quite accurately. There is a slight offset in the slopes and in the position

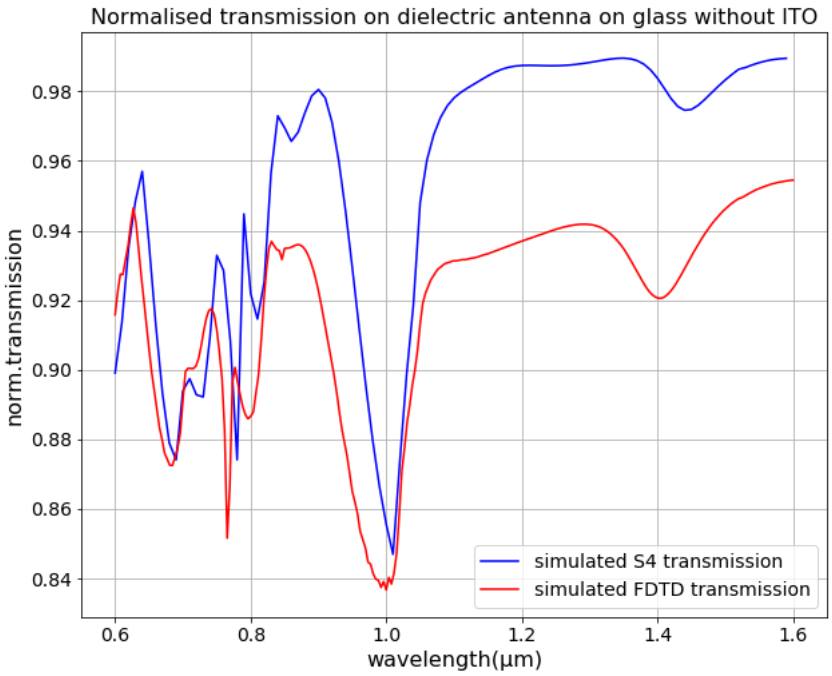

Figure 6: *Normalised transmission from one zirconia antenna on a glass spacer*

of the transmission dips in both graphs, but these can be dismissed as a by-product of the less accurate FMM method. We notice that the characteristic features of both gold and zirconia spectra are repeated in the S^4 simulation within a low error margin, making this a good approximation simulation. These graphs were simulated very quickly – in less than a minute – which is an immense improvement on the slow solution time of the FDTD method. In future, the matching of the spectra could be improved by simulation with a larger number of Fourier expansions for both structures.

5.2 Running the simulation with the ITO layer

Having checked that the S^4 software is operating correctly with simple structures, another control simulation had to be run to check how well the S^4 simulation recreates a reflection spectrum from a gold antenna with a layer of ENZ material. The wavelength sweep was chosen to include the ENZ wavelength range of the ITO (this is from 1.35 μm to 1.7 μm in this case). The ITO layer was initially located on top of the glass spacer, and the gold back-reflector is positioned underneath the glass spacer to facilitate reflection. A substrate is located underneath as the last layer, but this can in principle be made of any material with an arbitrary thickness, since no light will be travelling into this layer. For these simulations, 300 Fourier expansions was chosen as the standard to find a compromise between simulation time and accuracy.

As before, in this case we notice that in the S^4 simulated reflection the peaks occur at slightly different wavelengths, as well as not reaching the same height as the ones generated using FDTD.

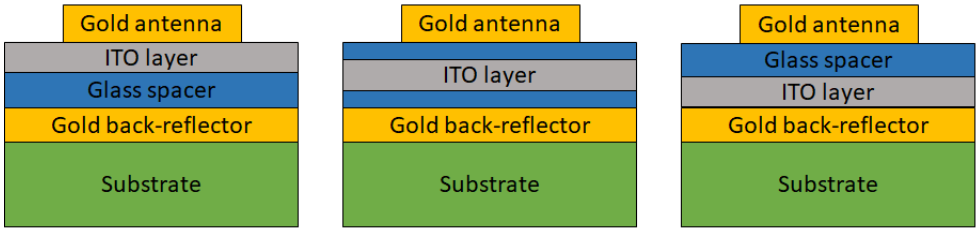

Figure 7: *Schematics of the structures used for simulations with the ITO layer*

However, we can still see that the characteristic peaks in the FDTD simulation have been reproduced by S^4, and that they have been matched to a fair degree of accuracy. Moreover, we must consider the position of the ITO layer in the structure: this layer also reflects, albeit not the same extent as the back-reflector, and thus some loss in amplitude of the reflected wave is expected. In **Figure 8**, we can see the effect of changing the position of the ITO layer within the structure. The reflection peaks produced when the ITO layer is underneath the glass spacer are greater in amplitude as opposed to those produced when the layer is above the spacer, and overall presents a better match to the FDTD simulation. We can thus already deduce that this would be the optimal choice for ENZ metasurfaces designed for reflectivity. Although this took longer to simulate than the previous examples – closer to an hour – this is still a fast result compared to FDTD simulations.

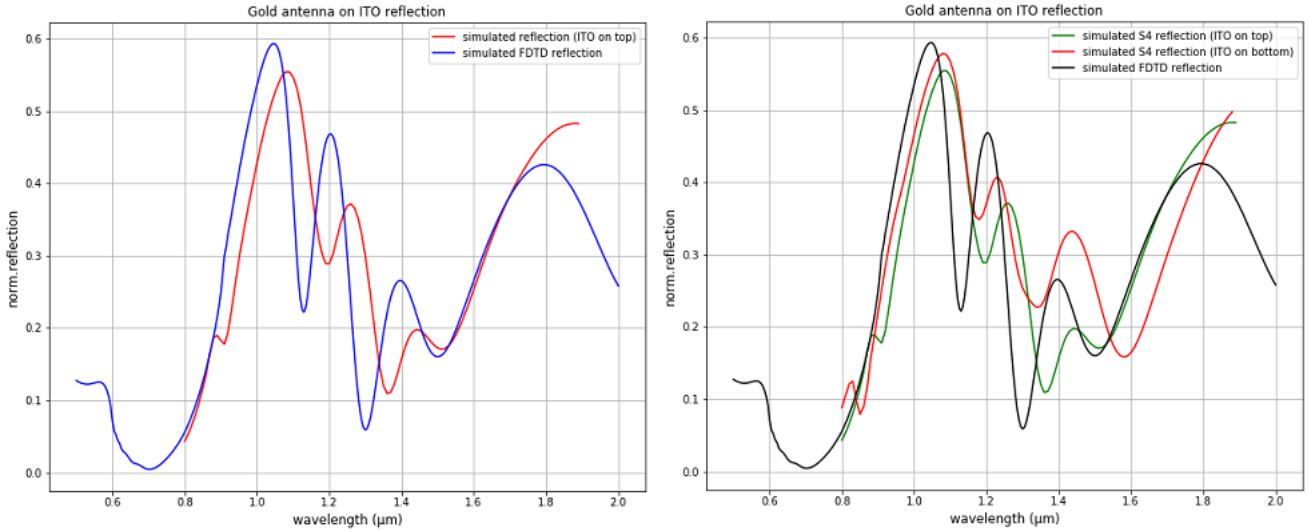

Figure 8: *Comparison of the S^4 and FDTD reflection spectra. Additionally, the right graph shows a simulation with the ITO placed underneath the glass spacer.*

5.3 Optimisation of design parameters

Since we have shown that S^4 simulations match their corresponding FDTD results well, we can now use the software to find the optimum dimensions and parameters for a variety of design purposes.

In this paper, the example of fibre optic cable is considered. Optical fibres experience some signal loss (attenuation) mostly in the form of absorption due to traces of water vapour present in the glass. To reduce this effect, optical fibres operate at certain wavelengths at which this attenuation is minimal – arguably the most effective such wavelength is at 1550 nm [14]. To optimise the design of optical fibres, ENZ metasurfaces can be incorporated into them to increase the reflectivity inside the fibre, thus increasing the transmission rate of the signal for long-distance communications, as well as other applications such as filters and sensors [15].

To achieve this, the ENZ metasurface has to be designed with a reflectivity peak at the corresponding wavelength. The peak has to have a normalised amplitude of 0.8 or above for the surface to be an effective reflector. Since this investigation is concerned with spectra from uncoupled antennae, care must be taken in setting the simulation region and antennae dimensions to ensure that there is no near-field coupling between antennae [16].

The changes to the dimensions and the parameters of the simulation were done by the method of trial and error: in future, it would be more effective to run sweeps for certain elements in a simulation at a time to obtain a wider range of results. It was found that decreasing the simulation region in the y-axis yielded a greater peak amplitude, and increasing the x-axis length of the gold antenna shifted the peak to a longer wavelength. To adjust for the change in antenna dimensions, the simulation region in the x-axis had to be increased as well. However, changing the y-axis length of the antenna gave more unpredictable results, and it was decided to let it remain as it was originally. It was found that adjusting the ITO layer thickness did not yield significant changes, and increasing the glass spacer layer only broadened the peak width. Increasing the antenna thickness slightly also helped to increase the amplitude of the peak. The table below outlines the optimal dimensions as found in this investigation:

Table of dimensions for gold antenna on metasurface		
Dimensions/μm	Original	Adjusted
Antenna x-length	0.42	0.67
Antenna y-length	0.169	0.169
Antenna thickness	0.04	0.06
ITO layer thickness	0.02	0.02
Glass spacer thickness	0.05	0.05
Gold back-reflector thickness	0.005	0.005
Simulation region	0.6 x 0.6	0.9 x 0.5

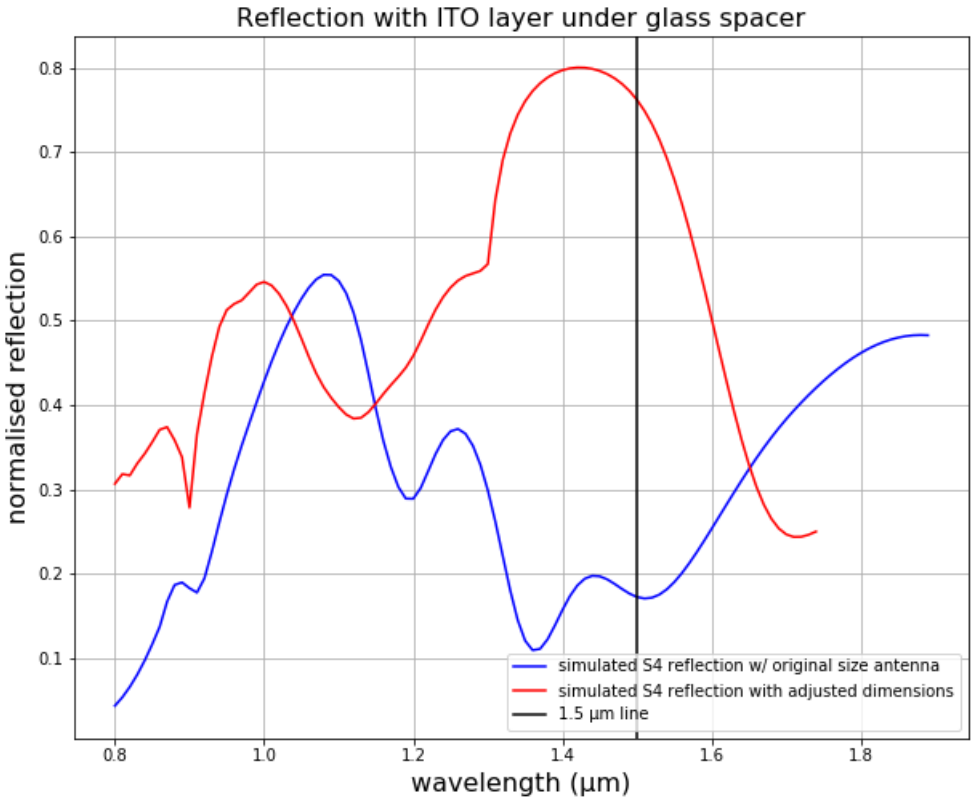

Figure 9: *Comparison of the reflection spectra from the original and adjusted simulations*

We notice from **Figure 9** that a suitable amplitude is achieved under the renewed parameters. However, the peak does not lie exactly on the optimal wavelength for optical fibre operation. This may be due to the inaccuracy of the software: we have seen before that the peaks of the S^4 simulation are slightly shifted to the analogous FDTD results. Conversely, more parameter changes have to be made in future to result in a better fit. A disadvantage of the S^4 software is that there is no automatic function to output the phase of the resulting wave relative to the incident, making it difficult to tell whether the incident and reflected waves interfere constructively or destructively. If the latter is the case, it would lead to loss of signal and less effective transmission along the optical fibre. In future investigations, the phase will have to be found manually by defining a new function within the program to calculate this. However, this is a significant result for the design process of ENZ metasurfaces, as the time taken to achieve these results is reduced significantly than if FDTD were to be used. The FDTD method can be used as a final step to obtain an accurate spectrum from the design dimensions found in the approximated S^4 simulation.

6 Conclusion

Overall, this investigation has found that S^4 is a useful software to help design ENZ metasurfaces. Although S^4 has its flaws, such as decreased accuracy and no automatic phase output, it can simulate good approximations that match the corresponding FDTD results. The greatest advantage of the S^4 software is the speed of simulation: several simulations can be launched at once from multiple CPU cores, and be completed in less than two hours, which is a significant improvement on FDTD simulation time. While the FDTD method will continue to be used to produce accurate and reliable simulations, the optimal dimensions and parameters for metasurface design can be quickly obtained via S^4, and the resulting spectra approximated to a good degree. If it is more widely used, S^4 has the potential to greatly accelerate the design process of ENZ metasurfaces, and this would pave the way to their becoming easily accessible, and their wider use in academia, industry, and technology.

7 Acknowledgments

I would like to sincerely thank my supervisor, Dr. Sebastian Schulz, and his PhD student, Laura Wynne, for the supervision, help, and guidance they provided throughout this research project. I would also like to thank Lord Laidlaw and the Laidlaw Foundation for funding and providing an opportunity to conduct this research. Finally, I would like to thank the University of St Andrews Laidlaw team for their continued support throughout the summer.

References

[1] *"Fundamentals of fibre optics in telecommunications and sensor systems"* edited by B.P. Pal, New Age International Publishers (1992)

[2] M. Kaiser, A. Yafi, M. Cinat, B. Choi, A. J. Durkin, *"Noninvasive assessment of burn wound severity using optical technology: A review of current and future modalities"*, Burns, **37**, 377-386 (2011)

[3] O. Reshef, I. De Leon, M.Z. Alam et al. *"Nonlinear optical effects in epsilon-near-zero media"* Nat. Rev. Mater. **4**, 535–551 (2019)

[4] M. H. Javani and M. I. Stockman, *"Real and imaginary properties of epsilon-near-zero-materials"*, Phys. Rev. Lett. **117**, 107404 (2016)

[5] Q. He, S. Sun, S. Xiao, L. Zhou, *"High Efficiency Metasurfaces: Principles, Realizations, and Applications"*, Advanced Optical Materials, **6**, 1800415 (2018)

[6] N. Yu, F. Capasso, *"Flat optics with designer metasurfaces"*, Nature Mater. **13**, 139–150 (2014)

[7] X. Wang, J. Ding, B. Zheng et al. *"Simultaneous Realization of Anomalous Reflection and Transmission at Two Frequencies using Bi-functional Metasurfaces"*, Sci. Rep. **8**, 1876 (2018)

[8] N. Anttu, H. Mäntynen, T. Sadi, A. Matikainen, J. Turunen and H. Lipsanen, *"Absorption modeling with FMM, FEM and FDTD"*, 2019 International Conference on Numerical Simulation of Optoelectronic Devices (NUSOD) (2019)

[9] K. L. Shlager, J. B. Schneider, *"A selective survey of the finite-difference time-domain literature"*, IEEE Antennas and Propagation Magazine, **37**, 4, 39-57, (1995)

[10] *"Fourier Modal Method and its Applications in Computational Nanophotonics"* by H. Kim, J. Park, B. Lee, CRC Press, Taylor and Francis Group (2012)

[11] V. Liu, S. Fan, *"S4: A free electromagnetic solver for layered periodic structures"*, Computer Physics Communications **183**, 2233-2244 (2012)

[12] P. B. Johnson, R. W. Christy, *"Optical Constants of the Noble Metals"*, Physical Review B, **6**, 4370-4379 (1972)

[13] D. L. Wood, K. Nassau, *"Refractive index of cubic zirconia stabilized with yttria"*, Appl. Opt. **21**, 2978-2981 (1982)

[14] M. C. Al Naboulsi, H. Sizun, F. de Fornel, *"Fog attenuation prediction for optical and infrared waves"*, Optical Engineering, **43** (2004)

[15] M. Guo, L. Huang, W. Liu, J. Ding, *"Hybrid metasurface comprising epsilon-near-zero material for double transparent windows in optical communication band"*, Optical Materials, **112** (2021)

[16] S. A. Schulz, A. A. Tahir, M. Zahirul Alam, J. Upham, I. De Leon, R. W. Boyd,*"Optical response of dipole antennas on an epsilon-near-zero substrate"* Phys. Rev. A, **93**, 063846 (2016)